УНИВЕРЗИТЕТ У БЕОГРАДУ - ГРАЂЕВИНСКИ ФАКУЛТЕТ
UNIVERSITY OF BELGRADE - FACULTY OF CIVIL ENGINEERING

УНИВЕРЗИТЕТ ЦРНЕ ГОРЕ - ГРАЂЕВИНСКИ ФАКУЛТЕТ
UNIVERSITY OF MONTENEGRO - FACULTY OF CIVIL ENGINEERING

АКАДЕМИЈА ИНЖЕЊЕРСКИХ НАУКА СРБИЈЕ
ACADEMY OF ENGINEERING SCIENCES OF SERBIA

ТЕОРИЈА ГРАЂЕВИНСКИХ КОНСТРУКЦИЈА

Монографија посвећена успомени на професора Миодрага Секуловића

THEORY OF CIVIL ENGINEERING STRUCTURES

Monograph dedicated to the memory of Professor Miodrag Sekulović

Уредници / Editors

Проф. др Живојин Прашчевић

Проф. др Раденко Пејовић

В. проф. др Ратко Салатић

В. проф. др Марија Нефовска-Даниловић

Београд, 2019.

Издавачи / Publishers
УНИВЕРЗИТЕТ У БЕОГРАДУ - ГРАЂЕВИНСКИ ФАКУЛТЕТ
UNIVERSITY OF BELGRADE - FACULTY OF CIVIL ENGINEERING

УНИВЕРЗИТЕТ ЦРНЕ ГОРЕ - ГРАЂЕВИНСКИ ФАКУЛТЕТ У ПОДГОРИЦИ
UNIVERSITY OF MONTENEGRO - FACULTY OF CIVIL ENGINEERING IN PODGORICA

АКАДЕМИЈА ИНЖЕЊЕРСКИХ НАУКА СРБИЈЕ
ACADEMY OF ENGINEERING SCIENCES OF SERBIA

За издавача / For the publisher
Проф. др Владан Кузмановић
Проф. др Марина Ракочевић
Проф. др Бранко Ковачевић

Уредници / Editors
Проф. др Живојин Прашчевић
Проф. др Раденко Пејовић
В. проф. др Ратко Салатић
В. проф. др Марија Нефовска-Даниловић

Рецензенти / Reviewers
Проф. др Ђорђе Лађиновић
Проф. др Александар Прокић

Техничка припрема / Technical preparation
В. проф. др Марија Нефовска-Даниловић
Доц. др Мирослав Марјановић
Емилија Дамњановић
Марија Милојевић

Дизајн корица / Cover design
Доц. др Мирослав Марјановић

Штампа / Printing
Бирограф, Земун

Тираж 300 примерака
Number of copies 300

ISBN 978-86-7518-208-5

Miroslav MARJANOVIĆ, Emilija DAMNJANOVIĆ

BENDING ANALYSIS OF CROSS-LAMINATED-TIMBER (CLT) PANELS USING LAYERED FINITE ELEMENTS

САВИЈАЊЕ ПАНЕЛА ОД УНАКРСНО-ЛАМЕЛИРАНОГ ДРВЕТА (CLT) ПРИМЕНОМ СЛОЈЕВИТИХ КОНАЧНИХ ЕЛЕМЕНАТА

Miroslav Marjanović, PhD Civil Eng.
Assistant Professor at the Faculty of Civil Engineering, University of Belgrade

Born in 1986, BSc in 2009, MSc in 2010 and PhD in 2016 at the Faculty of Civil Engineering, University of Belgrade. Presently, Assistant Professor in the field of Theory of Structures. Research fields: theory of composite plates and shells, FEM, nonlinear analysis of structures, structural vibration.

Emilija Damnjanović, MSc Civil Eng.
Teaching Assistant at the Faculty of Civil Engineering, University of Belgrade

Born in 1991, BSc in 2014 and MSc in 2015 at the Faculty of Civil Engineering, University of Belgrade. Presently, Teaching Assistant in the field of Theory of Structures. Research fields: theory of composite plates and shells, finite element and dynamic stiffness methods.

Summary

Cross-laminated timber panels are composite wood products with an increasing application in civil engineering. The low environmental impact and high mechanical performance encourage the use of CLT in modern buildings instead of traditional mineral-based building materials. The complex CLT-specific material characteristics, characterized by the high shear deformations across the plate thickness, complicate an accurate kinematic description of CLT. The traditional computational models used in standards for design of timber structures are generally based on beam theories, limiting the design approaches to slender panels. Therefore, the application of complex numerical models is required for a more intensive use of CLT.

In the paper, the full layerwise theory of Reddy served as a basis for the formulation of layered quadrilateral finite elements for the analysis of CLT panels. Original procedure for post-processing of stresses is presented. The model is validated against the numerical and experimental data in the literature. Excellent agreement is achieved.

Keywords: cross-laminated timber, finite element, layerwise theory

Резиме

Панели од унакрсно ламелираног дрвета (CLT) су композитни производи чија примена у грађевинарству је све већа. Мали утицај на животну средину и добре механичке карактеристике доводе до примене CLT панела у модерним зградама, уместо традиционалних (минералних) грађевинских материјала. Сложене материјалне карактеристике специфичне за CLT, које одликују високе смичуће деформације по дебљини панела, компликују прецизно описивање кинематике CLT панела. Традиционални прорачунски модели, примењени у стандардима за прорачун дрвених конструкција, генерално се заснивају на теоријама греде и ограничени су на танке панеле. Са тим у складу, примена сложених нумеричких модела неопходна је за повећану примену CLT панела.

У овом раду, Reddy-ева слојевита теорија плоча била је основ за формулисање слојевитих четвороугаоних коначних елемената за анализу CLT панела. Дата је оригинална процедура за прорачун напона. Прецизност модела је потврђена поређењем са нумеричким и експерименталним подацима из литературе, и добијено је одлично поклапање резултата.

Кључне речи: унакрсно ламелирано дрво, коначни елемент, слојевита теорија

1. INTRODUCTION

Cross-laminated timber (CLT) panels are composite wood products with an increasing application in civil engineering during the last decade [1]. The low environmental impact and high mechanical performance encourage the use of CLT in modern residential and commercial buildings, instead of traditional mineral-based materials [2]. CLT panels consist of several (3, 5 or 7) laminas stacked and glued together in the cross-ply manner. Each layer has a thickness of 6-51 mm [3, 4] while the total thickness of commercial products is usually up to 300 mm. These structural elements usually have the span (l) and the width (b) up to 15 m and 3 m, respectively. Their thick and orthogonal structure, providing the considerable stiffness with the low weight, allows the application as full size walls or floors [5]. Finally, the ease of assembly allows prefabrication and reduces construction time and cost.

Wood is an orthotropic material with three principal material axes: the first one is aligned with the fiber or trunk direction (L), while the remaining two axes are orthogonal to the annual rings (radial direction – R and tangential direction - T). The principal material axes are shown in Figure 1. The orthotropic elastic material behavior of wood and the crosswise lay-up yield a relatively complex deformation behavior of CLT. The high ratio of modulus of elasticity in fiber direction (E_L) of lengthwise layers and the corresponding transverse shear modulus of the cross layers (rolling shear modulus G_{RT}) provokes high shear deformations across the plate thickness. The transverse shear strains γ_{xz} and γ_{yz} show considerable discontinuities at layer interfaces, while transverse shear stresses τ_{xz} and τ_{yz} are continuous and strongly nonlinear across the plate thickness. The above CLT-specific material characteristics complicate an appropriate and accurate kinematic description of cross-laminated timber. For an intensive and safe use of CLT, the challenges in the design phase require the application of complex numerical models.

Current design models for CLT mainly emerged from the long tradition of using only simple one-dimensional elements in wood structures. These models are generally based on different beam theories. Application of simple laminated beam theory is the most straightforward approach, but it neglects transverse shear effects [6]. The γ-method [7] allows the analysis of compliantly joined beams by introducing a correction factor to the bending stiffness. The shear analogy method [8, 9] is based on the separation of the two parts of overall bending stiffness of CLT: the individual stiffnesses of the lamellae and the stiffness increments by their joint action. However, beam theoretical approaches are not able to account for two-dimensional load transfer and, thus, cannot reflect the load carrying mechanism of a plate-like structure. These approaches are limited to slender panels (with a single pronounced load bearing direction).

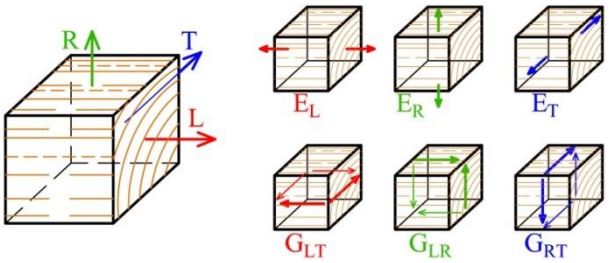

Figure 1. Principal material directions, elastic and shear moduli of wood

Two-dimensional approaches are conventionally applied through the applications of equivalent-single-layer (ESL) laminate theories [10-13]. The application of ESL theories is justified for the prediction of the global behavior of CLT (static deflections, critical buckling loads, fundamental vibration frequencies and mode shapes), and especially for slender laminates. In order to compensate for the incompatibility in the energetic balance, a shear correction factor is introduced in [11, 12]. However, if a highly accurate assessment of the stress-deformation state of the CLT is needed (for example, in localized regions around point supports, or simply in the case of very thick structural member) the use of refined laminate theories is recommended. The extensive review of refined laminate theories can be found in [14, 15], among others. Classical exact solutions for composite laminates in cylindrical bending developed by Pagano [16] could be successfully applied for standard thin CLT panels. The application of partial layerwise laminate theories has been authors' focus in development of response of previously damaged composite laminates [17-19]. Further incorporation of the transverse normal stress σ_z, as proposed in Full-Layerwise Plate Theory (FLWT) [20] is important in modeling the localized effects such as holes, cut-outs or stress-deformation state around point supports (σ_z is significant in these regions). The use of FLWT is justified also due to the capability to account for continuous transverse (interlaminar) stresses τ_{xz}, τ_{yz} and σ_z at layer interfaces, which is not possible in ESL theories. This satisfies the continuity conditions between the stress fields of the adjacent layers in the laminate.

In the paper, the full layerwise theory of Reddy [20] (FLWT) served as a basis for the development

of two layered quadrilateral finite elements (Q4 and Q8) for the analysis of CLT, accounting for the layerwise expansion of all three displacement components. Original procedure for post-processing of stresses is presented. The computational model is implemented using original object-oriented MATLAB [21] code, while the GUI for pre- and post-processing is developed using GiD [22]. The presented approach is validated against the available numerical and experimental data in the literature, and excellent agreement is achieved. Great potential for the use of the proposed model in the analysis of CLT is demonstrated.

2. LAYERWISE THEORY FOR BENDING ANALYSIS OF CLT PANELS

In the paper, we consider CLT panels made of n orthotropic layers. The total plate thickness is denoted as h (see Figure 2), while the thickness of the k^{th} lamina is denoted as h_k. The plate is supported along the portion Γ_u of the boundary Γ and loaded with loadings $q_t(x,y)$ and $q_b(x,y)$ acting to either top or the bottom surface of the plate (S_t or S_b).

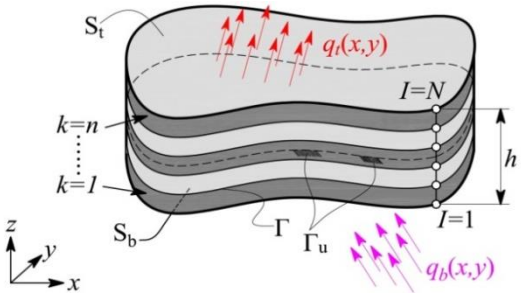

Figure 2. Laminated composite plate with n material layers and N numerical interfaces

Piece-wise linear variation of all three displacement components through the plate thickness is imposed, leading to the 3D stress description of all material layers. The displacement field of an arbitrary point (x,y,z) of the laminate is given as:

$$\begin{aligned} u(x,y,z) &= \sum_{I=1}^{N} U^I(x,y)\Phi^I(z) \\ v(x,y,z) &= \sum_{I=1}^{N} V^I(x,y)\Phi^I(z) \\ w(x,y,z) &= \sum_{I=1}^{N} W^I(x,y)\Phi^I(z) \end{aligned} \tag{1}$$

In Eq. (1), $U^I(x,y)$, $V^I(x,y)$ and $W^I(x,y)$ are the displacement components in the I^{th} numerical layer of the plate in directions x, y and z, respectively, while N is the number of interfaces between the layers including S_t and S_b. $\Phi^I(z)$ are selected to be linear layerwise continuous functions of the z-coordinate, and they are given in [20].

The linear strain field associated with the previously shown displacement field can be found in [20]. It serves as the basis for the derivation of $3N$ governing differential equations which define the strong form of the FLWT. To reduce the 3D model to the 2D, the z-coordinate is eliminated by the explicit integration of stress components multiplied with the corresponding functions $\Phi^I(z)$, introducing the stress resultants which can be found in [20].

The stresses in the k^{th} layer are computed from the well-known lamina constitutive equations, while the laminate constitutive relations are derived by integrating the lamina constitutive equations through the thickness of the plate. The system of $3N$ Euler-Lagrange governing equations of motion for the FLWT are derived using the principle of virtual displacements, by satisfying the equilibrium of the virtual strain energy δU and the work done by the applied forces δV:

$$\begin{aligned} &\frac{\partial N_{xx}^I}{\partial x} + \frac{\partial N_{xy}^I}{\partial y} - Q_x^I = 0 \\ &\frac{\partial N_{xy}^I}{\partial x} + \frac{\partial N_{yy}^I}{\partial y} - Q_y^I = 0 \\ &\frac{\partial Q_x^I}{\partial x} + \frac{\partial Q_y^I}{\partial y} - \tilde{Q}_z^I + q_b\delta_{I1} + q_t\delta_{IN} = 0 \end{aligned} \tag{2}$$

where $N_{xx}^I, N_{xy}^I, N_{yy}^I, Q_x^I, Q_y^I, \tilde{Q}_z^I$ are stress resultants defined in [20], while δ_{I1} and δ_{IN} are displacement vectors at interfaces S_b and S_t, respectively.

3. FINITE ELEMENT MODEL

Based on the FLWT, the displacement finite element model (weak form) is derived by substituting an assumed interpolation of the displacement field into the equations of motion of the FLWT. The layered finite elements require only C0 continuity of the generalized displacements along element boundaries, because only translational displacement components are adopted as the nodal degrees of freedom. Out of plane coordinate has been eliminated in the calculation after the explicit integration of the displacement field in out-of-plane direction. This allows the formulation of the family of 2D layered (plate) finite elements. This allows for the 2D data structure which provides the following advantages against the conventional 3D models:

- the amount of input data is reduced,

- the out of plane interpolation can be refined independently of the in-plane one,
- Model reduction to a 2D one results in the computational savings while constructing the FE stiffness matrix.

All displacement components are interpolated as:

$$U^I(x,y)=\sum_{j=1}^{m}U_j^I\psi_j(x,y)$$
$$V^I(x,y)=\sum_{j=1}^{m}V_j^I\psi_j(x,y) \quad (3)$$
$$W^I(x,y)=\sum_{j=1}^{m}W_j^I\psi_j(x,y)$$

In Eq. 3, m is the number of nodes per element, U_j^I, V_j^I, W_j^I are the nodal values of displacements U^I, V^I and W^I in the j^{th} element node representing the behaviour of the laminated composite plate in the I^{th} numerical interface. Finally, $\psi_j(x,y)$ are 2D Lagrange interpolation polynomials associated with the j^{th} element node. The strain field is interpolated in the usual manner, by incorporating Eq. 3 in the kinematic relations of the FLWT (Eq. 2).

The matrix form of the FE model is obtained as:

$$\left[K^{IJ}\right]\left\{\Delta^I\right\}=\left\{F^I\right\} \quad (4)$$

In Eq. 4, $[K^{IJ}]$ is the element stiffness matrix, $\{\Delta^I\}$ is the element displacement vector and $\{F^J\}$ is the element force vector, I=1,…,N and J=1,…,N. $[K^{IJ}]$ is obtained using 2-D Gauss-Legendre quadrature for quadrilateral domains. Linear Q4 and quadratic serendipity Q8 layered quadrilateral elements have been considered. To avoid shear locking, reduced integration is used (2×2 points for Q8 and 1×1 point for Q4). After the derivation of characteristic element matrices, the assembly procedure is done in a usual manner. After the assembly procedure, the mathematical model on the structural level is obtained as **Kd** = **f**, where **K**, **d** and **f** are system stiffness matrix and system displacement and force vectors.

4. POST-COMPUTATION OF STRESSES

The assumed piecewise linear interpolation of displacement field through the laminate thickness provide discontinuous stresses across the interface between adjacent layers. Once the nodal displacements are obtained, the stresses at the top (t) and bottom (b) interfaces of the k^{th} lamina can be computed from the constitutive relations:

$$\begin{Bmatrix}\sigma_x\\ \sigma_y\\ \sigma_z\\ \tau_{xy}\end{Bmatrix}_b^k=\begin{bmatrix}\bar{C}_{11} & \bar{C}_{12} & \bar{C}_{16}\\ \bar{C}_{21} & \bar{C}_{22} & \bar{C}_{26}\\ \bar{C}_{31} & \bar{C}_{32} & \bar{C}_{36}\\ \bar{C}_{61} & \bar{C}_{62} & \bar{C}_{66}\end{bmatrix}^k\sum_{j=1}^{m}\begin{bmatrix}\psi_{j,x} & 0\\ 0 & \psi_{j,y}\\ \psi_{j,y} & \psi_{j,x}\end{bmatrix}\begin{Bmatrix}U\\ V\end{Bmatrix}_j^I+\begin{Bmatrix}\bar{C}_{13}\\ \bar{C}_{23}\\ \bar{C}_{33}\\ \bar{C}_{63}\end{Bmatrix}\sum_{j=1}^{m}\psi_j\left(W_j^{I+1}-W_j^I\right)\frac{1}{h_k}$$

$$\begin{Bmatrix}\sigma_x\\ \sigma_y\\ \sigma_z\\ \tau_{xy}\end{Bmatrix}_t^k=\begin{bmatrix}\bar{C}_{11} & \bar{C}_{12} & \bar{C}_{16}\\ \bar{C}_{21} & \bar{C}_{22} & \bar{C}_{26}\\ \bar{C}_{31} & \bar{C}_{32} & \bar{C}_{36}\\ \bar{C}_{61} & \bar{C}_{62} & \bar{C}_{66}\end{bmatrix}^k\sum_{j=1}^{m}\begin{bmatrix}\psi_{j,x} & 0\\ 0 & \psi_{j,y}\\ \psi_{j,y} & \psi_{j,x}\end{bmatrix}\begin{Bmatrix}U\\ V\end{Bmatrix}_j^{I+1}+\begin{Bmatrix}\bar{C}_{13}\\ \bar{C}_{23}\\ \bar{C}_{33}\\ \bar{C}_{63}\end{Bmatrix}\sum_{j=1}^{m}\psi_j\left(W_j^{I+1}-W_j^I\right)\frac{1}{h_k}$$

$$\begin{Bmatrix}\tau_{yz}\\ \tau_{xz}\end{Bmatrix}_b^k=\begin{bmatrix}\bar{C}_{44} & \bar{C}_{45}\\ \bar{C}_{54} & \bar{C}_{55}\end{bmatrix}^k\sum_{j=1}^{m}\begin{Bmatrix}\psi_{j,x}\\ \psi_{j,y}\end{Bmatrix}W_j^I+\begin{bmatrix}\bar{C}_{44} & \bar{C}_{45}\\ \bar{C}_{54} & \bar{C}_{55}\end{bmatrix}^I\sum_{j=1}^{m}\begin{bmatrix}\psi_j & 0\\ 0 & \psi_j\end{bmatrix}\left(\begin{Bmatrix}U\\ V\end{Bmatrix}_j^{I+1}-\begin{Bmatrix}U\\ V\end{Bmatrix}_j^I\right)\frac{1}{h_k} \quad (5)$$

$$\begin{Bmatrix}\tau_{yz}\\ \tau_{xz}\end{Bmatrix}_t^k=\begin{bmatrix}\bar{C}_{44} & \bar{C}_{45}\\ \bar{C}_{54} & \bar{C}_{55}\end{bmatrix}^k\sum_{j=1}^{m}\begin{Bmatrix}\psi_{j,x}\\ \psi_{j,y}\end{Bmatrix}W_j^{I+1}+\begin{bmatrix}\bar{C}_{44} & \bar{C}_{45}\\ \bar{C}_{54} & \bar{C}_{55}\end{bmatrix}^I\sum_{j=1}^{m}\begin{bmatrix}\psi_j & 0\\ 0 & \psi_j\end{bmatrix}\left(\begin{Bmatrix}U\\ V\end{Bmatrix}_j^{I+1}-\begin{Bmatrix}U\\ V\end{Bmatrix}_j^I\right)\frac{1}{h_k}$$

In Eq. 5, $\bar{C}_{ij}$ are the transformed elastic coefficients in the laminate (x,y,z) coordinates [20], while $\psi_{j,x}$ and $\psi_{j,x}$ denotes differentiation of Lagrange shape functions by x and y, respectively. Since the interlaminar stresses calculated in this way does not satisfy continuous distribution through the laminate thickness, they are post-processed by assuming the quadratic distribution within each layer k for every stress component:

$$\bar{\boldsymbol{\tau}}^k=\left\{\bar{\tau}_{xz}^k \quad \bar{\tau}_{yz}^k \quad \bar{\sigma}_z^k\right\}=a_{ij}^k\bar{z}^2+b_{ij}^k\bar{z}+c_{ij}^k \quad (6)$$

where k = 1,2,…,N and ij = xz, yz or zz.

This requires $3N$ equations for each of interlaminar stresses:

- satisfying the traction boundary conditions at S_b and S_t (2 equations)

$$\bar{\tau}^1\left(\bar{z}=0\right)=q_b, \qquad \bar{\tau}^N\left(\bar{z}=h_N\right)=q_t \tag{7a}$$

- providing the continuity of interlaminar stresses along interfaces *(N-1* equations)

$$\bar{\tau}^{k-1}\left(\bar{z}=h_{k-1}\right)=\bar{\tau}^k\left(\bar{z}=0\right) \tag{7b}$$

- assuming the interlaminar stresses from the constitutive equations to be an average interlaminar stresses within a considered layer (*N* equations)

$$\int_0^{h_k}\bar{\tau}^k\left(\bar{z}\right)d\bar{z}=\frac{\tau_b^k+\tau_t^k}{2}h_k \tag{7c}$$

- computing the jump in interlaminar stresses at each interface utilizing the 3D stress equations of equilibrium (*N-1* equations)

$$\frac{\partial\bar{\tau}^{k-1}_{(\bar{z}=h_{k-1})}}{\partial\bar{z}}-\frac{\partial\bar{\tau}^{k}_{(\bar{z}=0)}}{\partial\bar{z}}=\frac{\partial\tau^{3D,k-1}}{\partial z}-\frac{\partial\tau^{3D,k}}{\partial z} \tag{7d}$$

where $\boldsymbol{\tau}^{3D}=\left\{\tau_{xz}^{3D}\quad\tau_{yz}^{3D}\quad\sigma_{zz}^{3D}\right\}^T$ is the vector of interlaminar stresses, obtained from the additional 3D equilibrium equations:

$$\begin{aligned}&\tau_{xz,z}^{3D}=-\left(\sigma_{xx,x}+\tau_{xy,y}\right),\quad \tau_{yz,z}^{3D}=-\left(\tau_{xy,x}+\sigma_{yy,y}\right)\\&\sigma_{zz,z}^{3D}=-\left(\tau_{xz,x}+\tau_{yz,y}\right)\end{aligned} \tag{8}$$

5. MODEL VALIDATION

Example 1. The goal of the first example is to validate the proposed numerical model through the computational analysis of thick CLT panels. The focus is on the accurate representation of the 3D stress distribution through the thickness of the CLT panel. Thick panels are considered in order to highlight the inadequacy of ESL-based models for the accurate prediction of 3D stress state. The panels are simply supported along all sides in order to compare the obtained results against the Navier solutions based on both classical (CPT) and first-order shear deformation laminate theories (FSDT), and the exact solution by Pagano [16]. The benchmark results are extracted from [5]. 25×25 Fourier terms were considered for analytical solutions.

In the example, two simply supported square (*a*=*b*) CLT panels are analyzed (see Figure 3). The first panel is composed of three layers, having the thickness $h = [h_0/h_{90}/h_0] = [26/40/26] = 92$mm. The side length of the panel is $a = b =$ 920 mm (a/h = 10). The second panel is a 5-layer one, having the thickness $h = [h_0/h_{90}/h_0/h_{90}/h_0] = [26/40/26/40/26] = 158$mm. The side length of the panel is $a = b =$ 1580 mm (a/h = 10).

Each layer is modeled as a C24 unidirectional lamina, with the following material properties: E_L = 11000 N/mm^2, $E_T = E_R$ = 370 N/mm^2, $G_{LT} = G_{LR}$ = 690 N/mm^2, G_{RT} = 50 N/mm^2, ν_{LT} = 0.49, ν_{LR} = 0.39 and ν_{RT} = 0.64. The mechanical properties of CLT are adopted according to [5, 23].

Boundary conditions are prescribed in edge nodes: $U^1 = W^1 = 0$ for edge parallel to *x*-axis and $V^1 = W^1 = 0$ for edge parallel to *y*-axis. The panels are exposed to high distributed loads at the top surface, q_t = 350 kPa. The convergence study of the present model is performed using both Q4 and Q8 elements with reduced integration (to avoid shear locking). Two different mesh sizes are considered in both models: 6×6 and 10×10 for the first panel, and 10×10 and 16×16 elements for the second one. The laminas are modeled as single numerical layer, adopting the linear distribution of displacements along the lamina thickness.

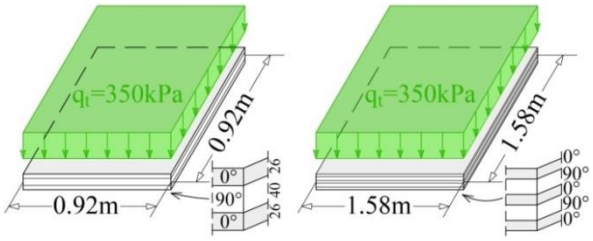

Figure 3. Considered 3- and 5-ply CLT panels

Figure 4 illustrates the distributions of: the in-plane displacement *u* at (0, *b*/2) and normal stresses σ_x and σ_y at (*a*/2, *b*/2) through the thickness of the 3-ply panel. The zig-zag shaped distribution of displacement *u* is achieved using FLWT for both elements and both considered mesh densities. This is in accordance with the exact solution [16].

For all considered models, two in-plane stress components σ_x and σ_y exhibit the correct discontinuous distribution, with considerably different slopes in soft and stiff layers. However, both CPT and FSDT theories underpredict the max normal stress σ_x, that may lead to design errors when dealing with the thick CLT panels. On the other hand, FLWT-based models have excellent agreement with the exact solution even for the coarse mesh and relatively simple (Q4) element type.

The considered transverse shear stresses τ_{xz} and τ_{yz} are plotted in Figure 5 along the thickness coordi-

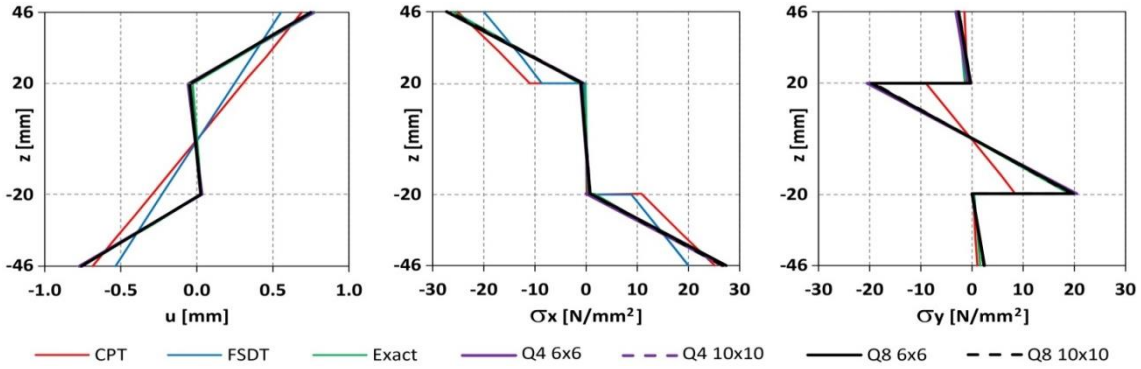

Figure 4. Distributions of the in-plane displacement u (0, b/2) and normal stresses σ_x and σ_y at (a/2, b/2) through the thickness of the 3-ply panel, considering different models, element types and mesh densities

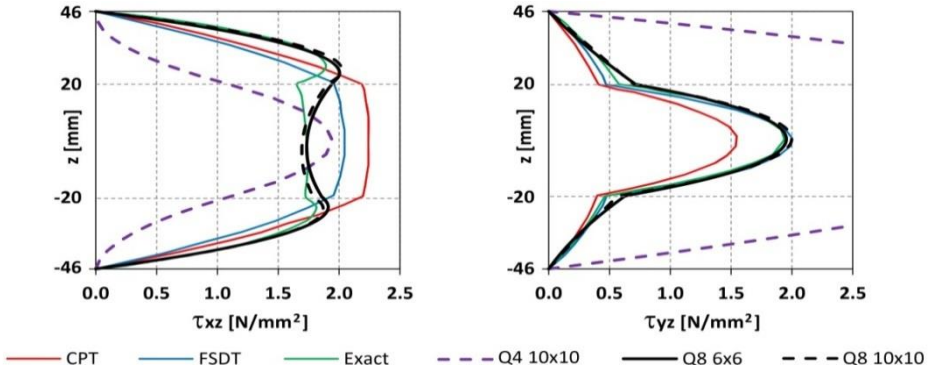

Figure 5. Distributions of the transverse shear stresses τ_{xz} (0, b/2) and τ_{yz} (a/2, 0) through the thickness of the 3-ply panel, considering different models, element types and mesh densities

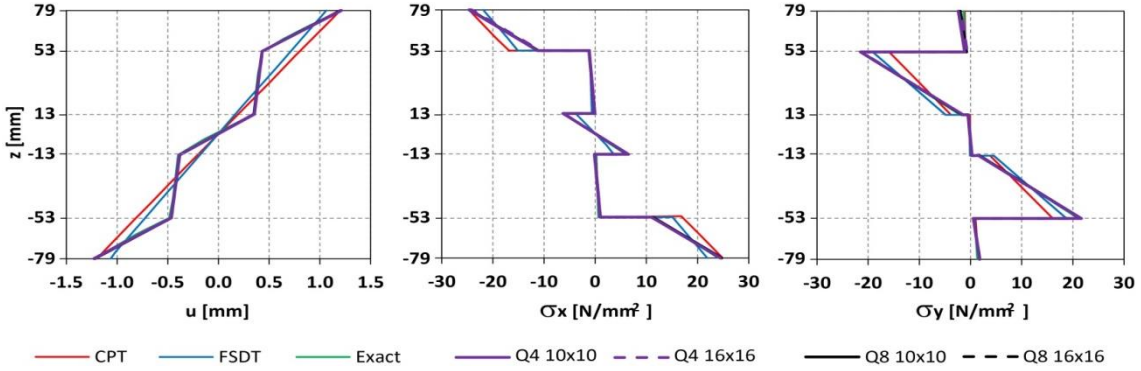

Figure 6. Distributions of the in-plane displacement u (0, b/2) and normal stresses σ_x and σ_y at (a/2, b/2) through the thickness of the 5-ply panel, considering different models, element types and mesh densities

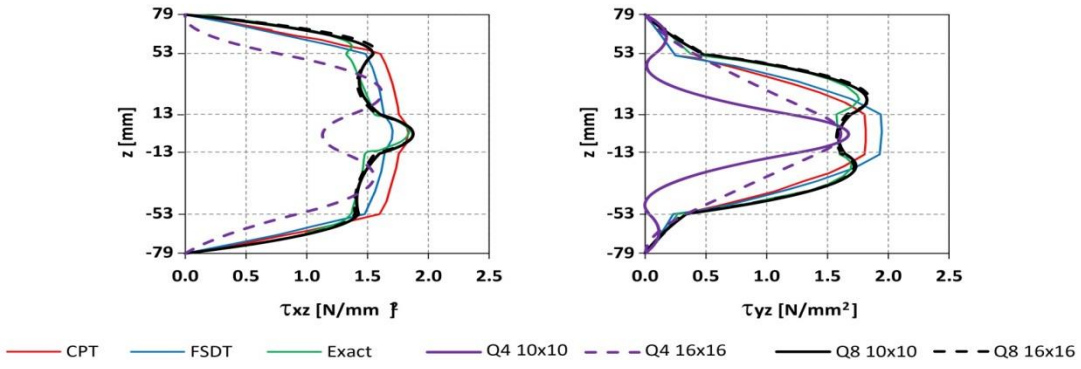

Figure 7. Distributions of the transverse shear stresses τ_{xz} (0, b/2) and τ_{yz} (a/2, 0) through the thickness of the 5-ply panel, considering different models, element types and mesh densities

nate z at the locations (0, b/2) and (a/2, 0), for the 3-ply panel. Obviously, ESL theories are unable to represent the correct distribution of τ_{xz} and τ_{yz} through the plate thickness. However, the transverse shear stress distributions obtained from both the exact solution and the Q8 finite element models based on FLWT exhibit the laminate-specific course. The slight asymmetry of transverse shear stresses obtained in the above solutions originates from the effect of the transverse normal stress σ_z which is disregarded in ESL plate theories. As indicated in [5], the discrepancies of out-of-plane shear strains γ_{xz} and γ_{yz} obtained using FSDT will lead the unrealistic results for the corresponding transverse shear stresses τ_{xz} and τ_{yz}, because these stress components are obtained using relatively simple Hooke's law formula adopted in classical standards for the design of timber structures.

Q4 (linear) elements based on FLWT cannot give the accurate prediction of the transverse shear stresses, due to the relatively low number of integration points used in the reduced integration of element stiffness matrices. On the contrary, Q8 elements are capable to predict the laminate-specific distribution of transverse shear stresses, with the slight overprediction. Mesh refinement lead to the convergence of results for τ_{xz} and τ_{yz} to the exact solution.

Figure 6 shows the distributions of u (0, b/2), σ_x (a/2, b/2) and σ_y (a/2, b/2) through the thickness of the 5-ply panel. Again, the zig-zag shaped distribution of u is achieved using FLWT. For the 5-ply panel, all considered models give accurate prediction of the max normal stresses σ_x and σ_y. Nevertheless, the ESL-based models are not completely matching the exact stress distribution, especially at layer interfaces.

The distribution of transverse shear stresses τ_{xz} and τ_{yz} at characteristic locations is depicted in Figure 7. While the ESL theories are unable to represent the correct distribution of τ_{xz} and τ_{yz}, the transverse shear stress distributions from the Q8 finite element models based on FLWT are in agreement with the exact solution. Again, the asymmetry originates from the effect of the transverse normal stress σ_z. Q4 FLWT elements fail in the prediction of the transverse shear stresses, while the Q8 elements are capable to predict the laminate-specific distribution of τ_{xz} and τ_{yz}.

Example 2. In the second example, experimental data from [24] is used to further validate the proposed model. Simply supported thin, square (a=b) CLT panels are considered, as shown in Figure 8. The panels have the following geometry: a = b = 2450mm, h = [h_0/h_{90}/h_0] = [10/50/10] = 70mm (a/h = 35). Each layer is modeled as a C24 unidirectional lamina. Two sets of material properties (see Table 1) are considered. The panels are exposed to concentrated loads of 30kN, on subareas of 150x150 mm². Two load layouts are considered: in the plate center (Q) and at four quarter points (4Q). Boundary conditions are prescribed in edge nodes: U^1=W^1=0 for edge parallel to x-axis and V^1=W^1=0 for edge parallel to y-axis. Two different mesh sizes are used: 17×17 and 32×32 finite elements.

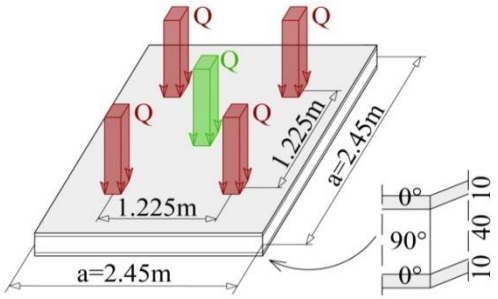

Figure 8. Layout of [10/50/10] mm CLT panel loaded with Q=30kN in plate center (green) and at four quarter points (red)

Table 1. Mechanical properties for two considered CLT panels of class C24

	Panel 1	Panel 2
E_L	11500 N/mm^2	12500 N/mm^2
E_T = E_R	575 N/mm^2	625 N/mm^2
G_{LT} = G_{LR}	720 N/mm^2	780 N/mm^2
G_{RT}	70 N/mm^2	80 N/mm^2
v_{LT}	0.49	
v_{LR}	0.39	
v_{RT}	0.64	

For the comparison, the mean experimental data [24] for the deflection w and the stress component σ_x are summarized in Tables 2 and 3, from the measurements on the three replicates of each plate set. In addition, set of results obtained using the analytical solution based on FSDT is extracted from [5] to compare the obtained results with these obtained using ESL-based model.

Table 2. Comparison of maximum deflections from different FE models against experimental [24] and Navier (FSDT) solution [5]

Load	**4Q**	**4Q**	**Q**	**Q**
Panel	**1**	**2**	**1**	**2**
w_{exp} [24]	33.8	30.2	20.9	18.2
w_{FSDT} [5]	34.1	31.4	20.9	19.2
Q4 17×17	31.13	28.6	18.56	17.02
Q4 32×32	31.29	28.75	19.28	17.68
Q8 17×17	31.01	28.49	18.61	17.06
Q8 32×32	31.26	28.72	19.24	17.64

Table 3. Comparison of normal stresses σ_x on the bottom side of CLT panels from different FE models, against experimental [24] and Navier (FSDT) solution [5]

Load	**4Q**	**4Q**	**Q**	**Q**
Panel	**1**	**2**	**1**	**2**
w_{exp} [24]	27.7	27.2	28.1	23.4
w_{FSDT} [5]	20.4	20.6	20.4	20.6
Q4 17×17	22.15	22.09	21.08	21.03
Q4 32×32	24.08	24.01	23.80	23.74
Q8 17×17	24.80	24.74	23.29	23.22
Q8 32×32	27.94	27.83	27.94	27.83

In terms of the deflection *w*, the proposed model gives slightly stiffer response of CLT panels in comparison with the experimental data. The average relative deviation from the measured data is -6.8%. Better agreement (-4.9%) is obtained for 4Q loading scheme, in comparison with Q (-8.6%). The obtained values are expectedly lower in comparison with FSDT, due to the more accurate consideration of transverse shear deformation. The average deviation is -9.1%.

As shown in [5], FSDT results for the normal stress σ_x are lower than the experimental data for about 20 %, even for very slender plates with an *a/h* ratio of 35, confirming that FSDT is unable to accurately predict the stress state in CLT under concentrated loading, due to neglecting of σ_z.

On the contrary, FLWT confirmed to give an accurate prediction of the normal stress σ_x directly under concentrated loading. However, the accuracy of results depends on mesh density and selected element type. As shown in [5], considerable deviations of the results obtained using FLWT from the measured data are only observed for Panel 2 under concentrated load in the plate center (see the last column in Tables 2 and 3). The plates of this set showed some variation of the elastic moduli measured at the bottom layers [5].

For other three sets of results, the average differences for the normal stress σ_x are: -21.3% for 17×17 Q4, -13.4% for 32×32 Q4, -12.2% for 17×17 Q8 and only -0.9% for 32×32 Q8 elements, showing the obvious convergence of results.

6. CONCLUSIONS

The application of Cross-laminated timber (CLT) panels is increasing during the last decade, due to the low environmental impact and high mechanical performance. The thick and orthogonal structure of CLT provides the considerable stiffness with the low weight, while the ease of assembly allows prefabrication and reduces construction time and cost.

The orthotropic behaviour of CLT is characterized by high shear deformations across the plate thickness. Transverse shear stresses τ_{xz} and τ_{yz} are continuous and strongly nonlinear across the plate thickness, which complicates an appropriate and accurate kinematic description of CLT. To overcome the above difficulties, the full layerwise theory of Reddy (FLWT) served as a basis for the development of Q4 and Q8 layered quadrilateral finite elements. To avoid shear locking, reduced integration is used. Starting from the layerwise expansion of all displacement components, FLWT is capable to calculate all components of the stress tensor, in contrary to the conventional equivalent-single-layer theories. The incorporation of the transverse normal stress σ_z is especially important, allowing the modeling of the localized effects such as holes, cut-outs or point supports.

The computational model is coded in MATLAB via object-oriented approach, while the GUI for pre- and post-processing is developed using GiD software. Original procedure for post-processing of stresses is presented. The formulated elements are applied in the computational bending analysis of 3-ply and 5-ply CLT panels. Both thick and slender panels are considered. From the conducted analyses, the following conclusions are derived:

- Both CPT and FSDT laminate theories underpredict the normal stress σ_x in thick CLT panels, in comparison with the exact solution. The differences are higher for the 3-ply than for the 5-ply panel, and they are highest at layer interfaces.
- The above plate theories are also unable to represent the correct distribution of τ_{xz} and τ_{yz} through the plate thickness.
- For slender CLT panels under concentrated loading, FSDT theory gives ~9% stiffer response in terms of deflections, when compared with the FLWT. The reason is the relatively simple consideration of transverse shear deformation by means of shear correction factor.
- FSDT results for the normal stress σ_x are lower than the experimental data for about 20 %, confirming that FSDT is unable to accurately predict the stress state in CLT under concentrated loading.
- In terms of the static deflection *w*, FLWT gives slightly stiffer response of CLT panels in comparison with the experimental data. Better agreement is obtained for 4Q

loading scheme, in comparison with the plate under center concentrated loading Q.

- FLWT-based models have excellent agreement of stress components σ_x and σ_y with the exact solution. Stresses exhibit the correct discontinuous distribution, with considerably different slopes in soft and stiff layers.
- FLWT also confirmed to give an accurate prediction of σ_x in slender CLT panels under concentrated loading. When compared to the measured experimental data, the accuracy of results depends on mesh density and selected element type. The average difference for σ_x is only -0.9% for fine mesh of Q8 elements, showing the obvious accuracy of the model.
- Q4 elements cannot give the accurate prediction of the transverse shear stresses, due to the relatively low number of integration points used in the reduced integration of element stiffness matrices. Q8 elements are capable to predict the distribution of transverse shear stresses.
- The slight asymmetry of transverse shear stresses obtained in the FLWT comes from the effect of the transverse normal stress σ_z which is disregarded in ESL plate theories.

ACKNOWLEDGMENTS

The financial support of the Ministry of Education, Science and Technological Development of the Republic of Serbia, through the projects TR-36046 and TR-36048, is acknowledged. The full license of GiD software is provided by the Institute for Structural Mechanics, Ruhr University Bochum.

REFERENCES

[1] L. Franzoni, A. Lebée, F. Lyon, G. Forêt. Elastic behavior of Cross Laminated Timber and timber panels with regular gaps: Thick-plate modeling and experimental validation. Engineering Structures, 141, 2017, 402–416.

[2] R. Brandner, D. Flatscher, A. Ringhofer, G. Schickhofer, A. Thiel. Cross Laminated Timber (CLT): overview and development. European Journal of Wood and Wood Products, 74(3), 2016, 331-351.

[3] EN 16351: timber structures – Cross Laminated Timber – requirements. European Committee of Standardization (CEN), Bruxelles, 2015.

[4] ANSI/APA PRG 320-2012. Standards for performance-rated cross-laminated timber. Tacoma, USA, 2012.

[5] R. Stürzenbecher, K. Hofstetter, J. Eberhardsteiner. Cross Laminated Timber: a multilayer, shear compliant plate and its mechanical behavior. 11th World Conference on Timber Engineering, Riva del Garda, Italy, 2010.

[6] H. Blass, P. Fellmoser. Design of solid wood panels with cross layers. 8th World Conference on Timber Engineering, Lahti, Finland, 2004.

[7] K. Möhler. Über das Tragverhalten von Biegeträgern und Druckstäben mit zusammengesetzten Querschnitten und nachgiebigen Verbindungsmittel. Habilitationsschrift, Technische Hochschule Karlsruhe, 1956.

[8] H. Kreuzinger. Platten, Scheiben und Schalen: Ein Berechnungsmodell für gängige Statikprogramme. Bauen Holz, 101(1), 1999, 34–39.

[9] H. Kreuzinger. Bemessung im Holzbau: Verbundkonstruktionen. Holzbau-Kalender 2002, Bruderverlag Karlsruhe, 2002, 598-621.

[10] G. Kirchhoff. Über das Gleichgewicht und die Bewegung einer elastischen Scheibe. Journal für reine und angewandte Mathematik, 40, 1850, 51-88.

[11] E. Reissner. The effect of transverse shear deformation on the bending of elastic plates. Journal of Applied Mechanics (ASME), 12(2), 1945, 69-79.

[12] R. Mindlin. Influence of rotator inertia and shear in flexural motions of isotropic elastic plates. Journal of Applied Mechanics, 18(1), 1951, 1031-1038.

[13] J. N. Reddy. A simple higher-order theory for laminated composite plates. Journal of Applied Mechanics, 51, 1984, 745-752.

[14] E. Carrera. Theories and finite elements for multilayered, anisotropic, composite plates and shells. Archives of Computational Methods in Engineering, 9(2), 2002, 87-140.

[15] E. Carrera. Historical review of zig-zag theories for multilayered plates and shells. Applied Mechanics Reviews, 56(3), 2003, 287-308.

[16] N. Pagano. Exact solutions for composite laminates in cylindrical bending. Journal of Composite Materials, 3(3), 1969, 398–411.

[17] M. Marjanović, Dj. Vuksanović. Layerwise solution of free vibrations and buckling of laminated composite and sandwich plates with embedded delaminations. Composite Structures, 108, 2014, 9-20.

[18] M. Marjanović, Dj. Vuksanović, G. Meschke. Geometrically nonlinear transient analysis of delaminated composite and sandwich plates using a layerwise displacement model with contact conditions. Composite Structures, 122, 2015, 67-81.

[19] M. Marjanović, G. Meschke, Dj. Vuksanović. A finite element model for propagating delamination in laminated composite plates based on the Virtual Crack Closure method. Composite Structures, 150, 2016, 8-19.

[20] J. N. Reddy. Mechanics of laminated composite plates and shells: theory and analysis. CRC Press, Boca Raton, Florida, USA, 2004.

[21] MATLAB R2011b. The MathWorks, Inc., Natick, Massachusetts, USA, 2011.

[22] GiD Customization Manual. CIMNE – International Center for Numerical Methods in Engineering, 2016.

[23] DIN 1052:2004: Design of timber structures – General rules and rules for buildings. Beuth Verlag, Berlin, Germany, 2004.

[24] C. Czaderski, R. Steiger, M. Howald, S. Olia, A. Gülzow, P. Niemz. Versuche und Berechnungen an allseitig gelagerten 3-schichtigen Brettsperrholzplatten. Holz als Roh- und Werkstoff, 65, 2007, 383-402.